



Open camera or QR reader and scan code to access this article and other resources online.

Lifelong Outcomes of Systemic Adeno-Associated Virus Micro-Dystrophin Gene Therapy in a Murine Duchenne Muscular Dystrophy Model

Nalinda B. Wasala,¹ Yongping Yue,¹ Bryan Hu,¹ Jin-Hong Shin,^{1,2} Arun Srivastava,^{3,†} Gang Yao,⁴ and Dongsheng Duan^{1,4-6,*}

Departments of ¹Molecular Microbiology and Immunology and ⁵Neurology, School of Medicine, The University of Missouri, Columbia, Missouri, USA; ²Department of Neurology, Pusan National University Yangsan Hospital, Yangsan, South Korea; ³Division of Cellular and Molecular Therapy, Child Health Research Institute, Department of Pediatrics, Department of Molecular Genetics and Microbiology, The University of Florida College of Medicine, Gainesville, Florida, USA; ⁴Department of Chemical and Biomedical Engineering, College of Engineering, The University of Missouri, Columbia, Missouri, USA; ⁶Department of Biomedical Sciences, College of Veterinary Medicine, The University of Missouri, Columbia, Missouri, USA.

Adeno-associated virus (AAV)-mediated systemic micro-dystrophin (μ Dys) therapy is currently in clinical trials. The hope is to permanently improve the life quality of Duchenne muscular dystrophy (DMD) patients. Numerous preclinical studies have been conducted to support these trials. However, none examined whether a single therapy at a young age can lead to lifelong disease amelioration. To address this critical question, we injected 1×10^{13} vg particles/mouse of an AAV serotype-9 μ Dys vector to 3-month-old mdx mice through the tail vein. Therapeutic outcomes were evaluated at the age of 11 months (adulthood, 8 months postinjection) and 21 months (terminal age, 18 months postinjection). Immunostaining and Western blot showed saturated supraphysiological levels of μ Dys expression in skeletal muscle and heart till the end of the study. Treatment significantly improved grip force and treadmill running, and significantly reduced the serum creatine kinase level at both time points. Since cardiac death is a major threat in late-stage patients, we evaluated cardiac electrophysiology and hemodynamics by ECG and the closed-chest cardiac catheter assay, respectively. Significant improvements were observed in these assays. Importantly, many ECG and hemodynamic parameters (heart rate, PR interval, QRS duration, QTc interval, end-diastolic/systolic volume, dP/dt max and min, max pressure, and ejection fraction) were completely normalized at 21 months of age. Our results have provided direct evidence that a single systemic AAV μ Dys therapy has the potential to provide lifelong benefits in the murine DMD model.

Keywords: DMD, micro-dystrophin, AAV, mdx, heart

INTRODUCTION

ADENO-ASSOCIATED VIRUS (AAV)-mediated micro-dystrophin (μ Dys) gene therapy is a promising approach to treat Duchenne muscular dystrophy (DMD), a lethal muscle-wasting disease in boys.¹ DMD is caused by the loss of a large cytoskeletal protein called dystrophin.² Dystrophin is expressed from the *DMD* gene, one of the largest genes in the genome.³ Mutations in the *DMD* gene

abolish dystrophin expression. As a monogenic disease, DMD is a perfect candidate for gene replacement therapy.

AAV has emerged as the most appealing vector for systemic gene therapy of neuromuscular diseases.^{4,5} One AAV drug has been approved by the Food and Drug Administration USA to treat spinal muscular atrophy.⁶ However, AAV is one of the smallest viruses.⁷ The maximum genome that can be efficiently packaged in the 25 nm AAV capsid is

*Correspondence: Dr. Dongsheng Duan, Department of Molecular Microbiology and Immunology, School of Medicine, The University of Missouri, One Hospital Drive, Columbia, MO 65212, USA. E-mail: duand@missouri.edu

[†]Correction added on May 11, 2023 after first online publication of May 2, 2023: Fifth author Arun Srivastava was mistakenly omitted in the originally published version of the article. The author by-line, affiliations, Authors' Contributions, Author Disclosure and Funding Information sections have been updated to reflect his contribution to the article.

~5 kb.^{8–10} The full-length *DMD* gene is ~2.4 mb. The full-length dystrophin coding sequence is ~11.4 kb. They greatly exceed the carrying capacity of the AAV vector. Although the engineered triple-AAV system can deliver a full-length dystrophin expression cassette, the efficiency is too low for therapy.¹¹ An alternative approach is to truncate the size of the dystrophin coding sequence.^{12,13} For the past two decades, numerous highly abbreviated microgenes were engineered.^{14–18} These minimized μ Dys genes are <4 kb and can be efficiently delivered with the AAV vector.¹⁹

Preclinical studies suggest that local and systemic AAV μ Dys gene therapy can effectively reduce muscle pathology and improve skeletal muscle and heart function (reviewed in Ref.¹⁹). Although these results have set a strong premise for ongoing human trials, lifelong follow-up studies are missing. DMD is a chronic disease and as such, an ideal therapy for DMD would be a single systemic delivery that can protect dystrophin-deficient muscles throughout life.

Long-term AAV persistence has been reported in normal human muscle.²⁰ However, whether this is the case in the dystrophic muscle remains unclear. To address this important question, we injected an AAV serotype-9 (AAV9) μ Dys vector into 3-month-old mdx mice through the tail vein at the dose of 1×10^{13} vector genome (vg) particles/mouse. The μ Dys-treated mice were followed until they reached the terminal age of 21 months.^{21,22} We examined μ Dys expression, serum creatine kinase (CK), grip force, treadmill running, ECG, and hemodynamic function of the heart. Immunostaining and Western blot revealed robust μ Dys expression in multiple limb muscles and heart. Serum CK level was significantly reduced. Skeletal muscle fibrosis was significantly decreased. Grip force and treadmill running distance were significantly improved. Multiple ECG and cardiac hemodynamic parameters were normalized. Our results suggest that a single systemic AAV μ Dys therapy may provide long-lasting benefits in mdx mice.

MATERIALS AND METHODS

Experimental animals

All animal experiments were approved by the institutional animal care and use committee and were in accordance with NIH guidelines. C57/BL10 (wild-type [WT] control) and dystrophin-deficient mdx mice were generated in a barrier facility using breeders purchased from The Jackson Laboratory (Bar Harbor, ME) (mdx, C57BL/10ScSn-*Dmd*^{mdx}/J, stock number 001801; BL10, C57BL/10ScSnJ, stock number 000476). Female mice were used in the study because aged female mdx mice are the only model that faithfully (both genetically and phenotypically) reproduced dilated cardiomyopathy in human patients.^{23,24} Since the median survival of female mdx mice is 21.25 months,²² we terminated treated mice at 21 months of age (range, 20.27–21.93 months; median, 21.77 months; mean \pm standard, 21.49 \pm 0.58 months). All mice were maintained in a specific-pathogen-free animal

care facility on a 12-h light (25 lux):12-h dark cycle with access to food and water *ad libitum*.

AAV production and delivery

The *cis* μ Dys packaging plasmid (also called SJ46 and Δ R2-15/ Δ R18-19/ Δ R20-23/ Δ C μ Dys) was published before.²⁵ It contained the N-terminal domain, hinge 1 (H1), spectrin-like repeat 1 (R1), R16, R17, H3, R24, H4, the cysteine-rich domain, and the Dys-2 epitope at the end of the dystrophin C-terminal domain. Transgene expression was regulated by the cytomegalovirus promoter and the simian virus 40 polyadenylation signal. The μ Dys construct was packaged in AAV9. Recombinant AAV vector was produced, purified, and titrated according to our published protocol.²⁶ A total of 1×10^{13} vg particles/mouse of the AAV9 μ Dys vector were injected through the tail vein to conscious 3-month-old mdx mice.

Morphological studies

Tissues were harvested at the end of the study. Harvested tissues were snap-frozen in the Tissue-Plus[®] optimal cutting temperature compound (Scigen Scientific, Gardena, CA, USA) in a liquid nitrogen-cooled 2-methylbutane bath. General histology was examined by hematoxylin and eosin (HE) staining. Fibrosis was examined by Masson trichrome (MT) staining. Dystrophin expression was evaluated by immunostaining using a monoclonal antibody that recognizes dystrophin H1-R1-R2 (NCL-Dys B, 1:80; Leica Biosystems, Product code DYSB, clone 34C5). Slides were viewed at the identical exposure setting using a Nikon E800 fluorescence microscope. Photomicrographs were taken with a Leica DFC7000 camera.

Fibrotic areas in the heart and skeletal muscle were quantified using the lasso tool in the Photoshop software on MT-stained whole tissue cross-section images. In brief, the micrometer scale was defined with the set measurement scale option in the software. The fibrotic area was marked using the quick selection tool. The sum of all fibrotic areas was then represented as a percentage of the whole cross-sectional area.

Western blot

To prepare for whole heart and muscle lysates, the tissues were snap-frozen in liquid nitrogen. The frozen tissue samples were ground to fine powder in liquid nitrogen followed by homogenization in a buffer containing 10% sodium dodecyl sulfate, 5 mM ethylenediaminetetraacetic acid, 62.5 mM Tris-HCl at pH6.8, and the protease inhibitor cocktail (Roche, Indianapolis, IN, USA). The crude lysate was chilled on ice for 2 min, and then centrifuged at 16,000 g for 2 min. The supernatant was collected as the whole muscle lysate. Protein concentration was measured using the DC protein assay kit (Bio-Rad, Hercules, CA, USA). The whole muscle lysate was heated at 95°C for 3 min to denature before loading in the gel.

Dystrophin was detected with a monoclonal antibody that recognizes the Dys-2 epitope at the C-terminal end of dystrophin (NCL-Dys2, 1:100; Leica Biosystems). Western blot was viewed using Li-Cor Odyssey Fc imaging system and quantification was performed using the LICOR Image Studio Version 5.0.21 software. The intensity of the respective protein band was normalized to the corresponding loading control in the same blot. The relative band intensity was further normalized to the WT control. Sarcomeric alpha-actinin was used as a loading control and was detected with a rabbit polyclonal antibody (1:2,000; Abcam, Cambridge, MA, USA).

Treadmill running

Treadmill endurance assay was performed as we described before with modifications.²⁷ In brief, mice were subjected to 5-day treadmill acclimation at a 7° uphill treadmill (Columbus Instruments, Columbus, OH, USA). The acclimation protocol begins with placing the animal on an unmoving flat treadmill for 2 min followed by 5 min in 7° uphill inclined treadmill for each day. All running acclimations were done at 7° inclined treadmill only. On the first day, the mouse ran at 5 m/min for 15 min followed by 10 m/min for 5 min. On day 2, the mouse ran at 5 m/min for 5 min, 10 m/min for 15 min, and 12 m/min for 5 min in that order. On day 3, the mouse ran at 5 m/min for 5 min, 10 m/min for 15 min, and 12 m/min for 10 min.

On days 4 and 5, the mouse ran for 5 m/min for 5 min, 10 m/min for 20 min, 12 m/min for 5 min, and 15 m/min for 5 min. The running distance was measured on day 6. On the day of distance measurement, the mouse was placed on an unmoving treadmill for 2 min and then ran at 5 m/min for 5 min. The treadmill speed was then increased by 1 m/min every 5 min. The total running distance was calculated after the mouse became exhausted. Exhaustion is diagnosed when the animal gives up running and ends up in contact with the shocker (at the minimal setting) for typically 1–3 s without attempting to re-enter the treadmill. Animals that did not run were excluded from the analysis.

Serum CK activity assay

Fresh serum was collected by tail vein bleeding. The CK activity was determined using the CK Liqui-UV test kit from Stanbio Laboratory (Boerne, TX, USA) according to the manufacturer's guidelines.

Forelimb grip strength measurement

Forelimb grip strength was measured with a computerized grip strength meter (Columbus Instruments) as we described previously.²⁸ The grip strength meter has a pulling bar attached to a force transducer and a digital display. The mouse was first acclimated to the apparatus for ~5 min. The mouse was then allowed to grab the pulling bar while being held from the tip of the tail. The mouse was gently pulled away from the grip bar. When the mouse can no longer grasp

the bar, the reading was recorded. The protocol was repeated five times with at least 30 s rest between trials. The highest three values were averaged to obtain the absolute grip strength. Normalized grip strength was obtained by dividing the absolute grip strength by the body weight.

ECG and hemodynamic assay

Cardiac functions were evaluated using our published protocols as described in the standard operating protocol in the *Cardiac Protocols for Duchenne Animal Models*.^{29,30,31} Specifically, a 12-lead ECG assay was performed using a commercial system from AD Instruments (Colorado Springs, CO, USA). The Q wave amplitude was determined using the lead I tracing. Other ECG parameters were analyzed using the lead II tracing.

The QTc interval was determined by correcting the QT interval with the heart rate. The cardiomyopathy index was calculated by dividing the QT interval by the PQ segment. Left ventricular hemodynamics was evaluated using a closed-chest approach as we previously described.²⁹ The resulting PV loops were analyzed with the PVAN software (Millar Instruments, Houston, TX, USA). The cardiac relaxation time constant Tau was calculated according to Weiss *et al.*³² The body surface area was calculated as described by Cheung *et al.*³³

Statistics

Data are presented as mean ± standard error of the mean. For all the physiological assays, data are presented using scatterplots. One-way analysis of variance (ANOVA) with Tukey's multiple comparison analysis was performed using GraphPad PRISM software version 7.0 for Mac OSX (GraphPad Software, La Jolla, CA, USA). A $p < 0.05$ was considered statistically significant.

RESULTS

Systemic therapy in young adult mice resulted in robust μ Dys expression in skeletal muscle and heart throughout life

To study the longitudinal effects of systemic AAV μ Dys gene therapy, we used a μ Dys construct that has been validated in murine and canine DMD models by local and systemic delivery.^{25,34–36} We packaged the μ Dys expression cassette in AAV9, a serotype that is currently being investigated in multiple clinical trials in DMD patients (NCT03362502, NCT04281485, and NCT05429372 sponsored by Pfizer; NCT03368742 sponsored by Solid Biosciences) (Fig. 1A).^{37–39} The μ Dys vector was injected into the tail vein of 3-month-old mdx mice at the dose of 1×10^{13} viral genome copies per animal (vg/mouse). Mice were euthanized at 21 months of age (Fig. 1A).

Immunostaining revealed saturated μ Dys expression at the sarcolemma in multiple limb muscles and the heart (Fig. 1B, D). Importantly, widespread μ Dys expression was achieved in muscles that are critical for respiration,

including the diaphragm, intercostal muscle, and abdominal muscle (Supplementary Fig. S1). On Western blots, the μ Dys level exceeded the level of full-length dystrophin in WT mice (Fig. 1C, E, Supplementary Fig. S2). On quantification, micro-dystrophin expression in the treated skeletal muscle and heart was ~ 9 - and ~ 2.5 -fold higher than that of full-length dystrophin in normal skeletal muscle and heart, respectively (right panels in Fig. 1C, E).

AAV9 μ Dys therapy reduced fibrosis in skeletal muscle and heart

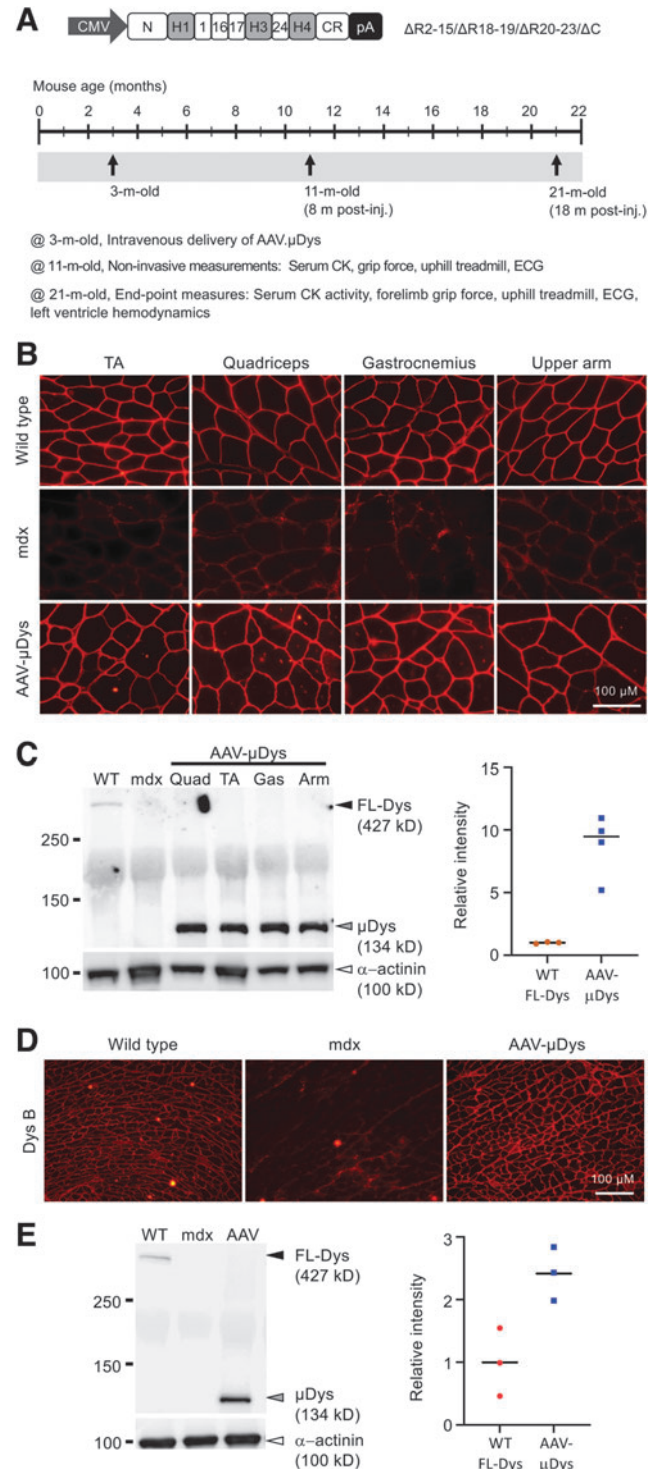
A hallmark of DMD is the replacement of muscle by noncontractile fibrotic tissue. We examined fibrosis by MT staining. On histochemical staining, the fibrotic replacement was clearly reduced in both heart and skeletal muscle (Fig. 2A, B; Supplementary Fig. S3). On quantification, $\sim 0.90\%$ of the heart area was fibrotic in μ Dys-treated mice (Fig. 2C). This was comparable with that of the normal heart. Quantification confirmed the reduction of fibrosis in the tibialis anterior muscle, but the difference did not reach statistical significance (Fig. 2D). We also examined the general histology by HE staining. Infiltrating mononucleated cells appeared greatly reduced in skeletal muscle and heart of μ Dys-treated mice (Fig. 2A, B; Supplementary Fig. S3A, C, E, and F). However, the percentage of myofibers with centrally located myonuclei did not change in μ Dys-treated mice (Fig. 2E).

AAV9 μ Dys therapy reduced serum CK, improved grip strength, and enhanced treadmill running

To quantify muscle damage, we evaluated serum CK activity (Fig. 3 top panels). The CK level was significantly increased in untreated mdx mice. Systemic μ Dys therapy significantly reduced the serum CK level at 8 and 18 months post-AAV delivery. Noninvasive grip force and treadmill

running were used to quantify gross muscle physiology at the middle and end of the study (Fig. 3 middle and bottom panels). Grip force was significantly enhanced and treadmill running distance was significantly increased when treated mice were examined at 11 months of age (8 months post-therapy) (Fig. 3A middle and bottom panels). Improvements in grip force and treadmill running lasted till 21

Figure 1. Single intravenous delivery of an AAV9 micro-dystrophin vector to 3-month-old mdx mice resulted in robust protein expression up to 18 months postinjection. **(A)** Top panel is a cartoon illustration of R2-15/ Δ R18-19/ Δ R20-23/ Δ C micro-dystrophin vector. Bottom panel shows the study plan. AAV [1×10^{13} viral genome particles (vg)/mouse] was injected at 3 months of age through the tail vein. Noninvasive assays were performed when animals were 11-month old (8 months postinjection). Terminal studies were performed when the animals reach 21 months of age (18 months postinjection). **(B)** Representative dystrophin immunofluorescence staining photomicrographs from different muscles, including the TA, quadriceps, gastrocnemius, and upper arm muscle. **(C)** Representative skeletal muscle Western blot. Quad, quadriceps; TA, tibialis anterior; Gas, gastrocnemius; Arm, upper arm muscle. Black arrowhead, full-length dystrophin; gray arrowhead, micro-dystrophin; white arrowhead, sarcomeric alpha-actinin (loading control). Densitometry quantification of the dystrophin level is shown in the scatterplot. **(D)** Representative dystrophin immunofluorescence staining photomicrographs of the heart. Dys B is the primary antibody used in the staining. Dys B recognizes H1-R1 region of the dystrophin protein. **(E)** Representative heart Western blot. Black arrowhead, full-length dystrophin; gray arrowhead, micro-dystrophin; white arrowhead, sarcomeric alpha-actinin (loading control). Densitometry quantification of the dystrophin level is shown in the scatterplot. AAV, adeno-associated virus; AAV9, AAV serotype-9; CMV, cytomegalovirus promoter; H1, hinge 1; R1, repeat 1; TA, tibialis anterior.



months of age (18 months post-therapy, the end of the study) (Fig. 3B middle and bottom panels).

AAV9 μ Dys therapy effectively prevented dilated cardiomyopathy in aged mdx mice

Heart function was examined by ECG and left-ventricle catheterization (Fig. 4; Supplementary Fig. S4). At 11 months of age, ECG examination showed significant improvements in PR interval, QRS duration, and cardiomyopathy index (Supplementary Fig. S4). Interestingly, nearly all ECG parameters (except for the Q amplitude) were normalized at 21 months of age in μ Dys-treated mdx mice (Fig. 4A). The hemodynamic function of the heart

was examined right before the mice were euthanized. Several systolic (end-systolic volume, dP/dt max, and maximum pressure) and diastolic (end-diastolic volume, dP/dt min, and heart relaxation constant Tau) parameters were fully normalized (Fig. 4B top two panels).

The ejection fraction of treated mice was significantly higher than that of untreated mdx mice (Fig. 4B bottom left panel). However, the stroke volume and cardiac output were not changed (Fig. 4B bottom middle and right panels). We also observed significant improvements in multiple other hemodynamics parameters, including the end-systolic

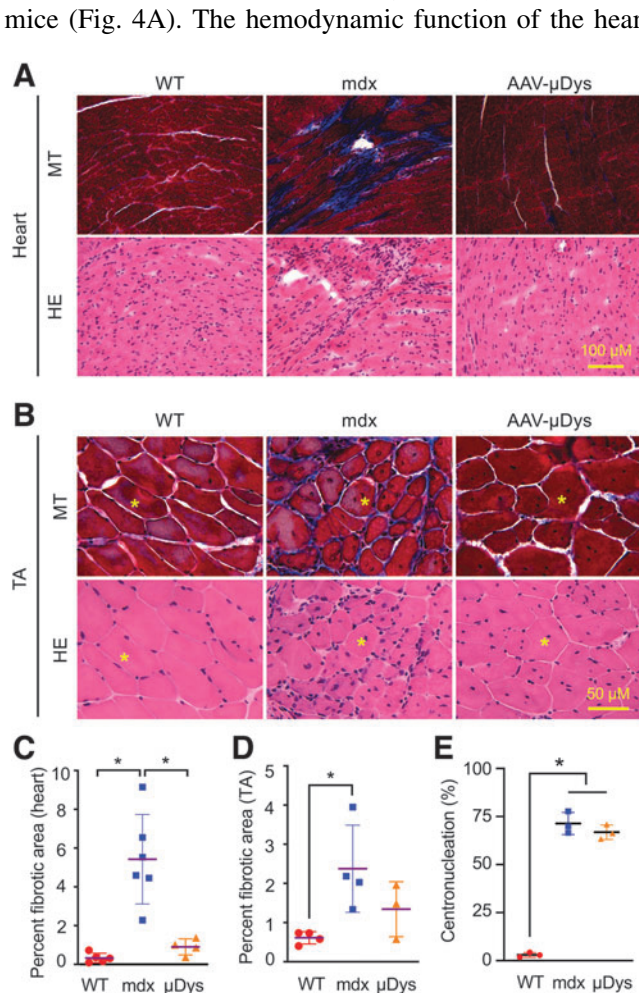


Figure 2. Long-term systemic AAV9 micro-dystrophin therapy significantly reduced fibrosis in heart and skeletal muscle. **(A)** Representative high-power photomicrographs from MT staining and HE staining of the heart of WT, mdx, and AAV9.micro-dystrophin (AAV- μ Dys)-treated mdx mice. Fibrotic tissue is stained in blue, and muscle is stained in dark red in MT staining. **(B)** Representative high-power photomicrographs from MT staining and HE staining of the TA muscle of WT, mdx, and AAV9.micro-dystrophin (AAV- μ Dys)-treated mdx mice. The yellow asterisk marks the same myofiber in serial sections. **(C)** Quantification of the fibrotic area in the heart (WT $n=5$, mdx $n=6$, AAV $n=4$). **(D)** Quantification of the fibrotic area in the TA muscle (WT $n=4$, mdx $n=4$, AAV $n=3$). **(E)** Quantification of the percentage of myofiber with centrally located nuclei in the TA muscle (WT $n=3$, mdx $n=3$, AAV $n=3$). *Significantly different from the indicated group(s), $p < 0.05$. HE, hematoxylin and eosin; MT, Masson trichrome; WT, wild type.

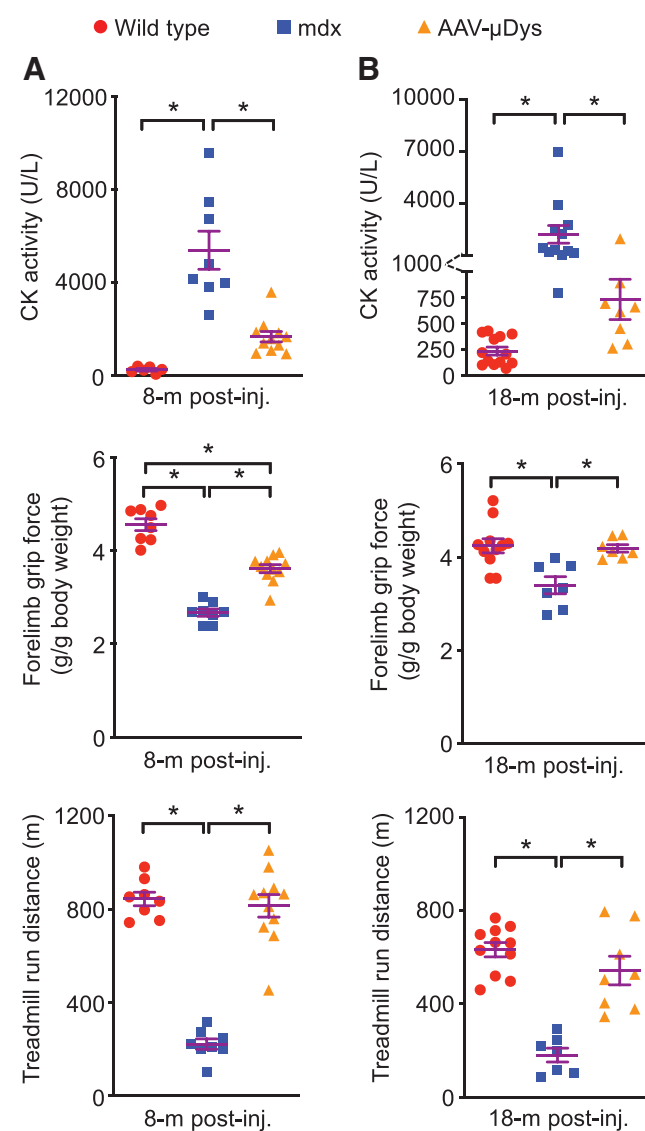


Figure 3. Long-term AAV9.micro-dystrophin therapy significantly reduced the serum CK level, and improved forelimb grip force and treadmill running distance. **(A)** Serum CK (WT $n=6$, mdx $n=8$, AAV $n=11$), grip force (WT $n=8$, mdx $n=8$, AAV $n=11$), and treadmill running distance (WT $n=8$, mdx $n=8$, AAV $n=11$) at 8 months post-AAV injection. **(B)** Serum CK (WT $n=13$, mdx $n=12$, AAV $n=8$), grip force (WT $n=11$, mdx $n=7$, AAV $n=7$), and treadmill running distance (WT $n=11$, mdx $n=7$, AAV $n=8$) at 18 months post-AAV injection. *Significantly different from the indicated group, $p < 0.05$. CK, creatine kinase.

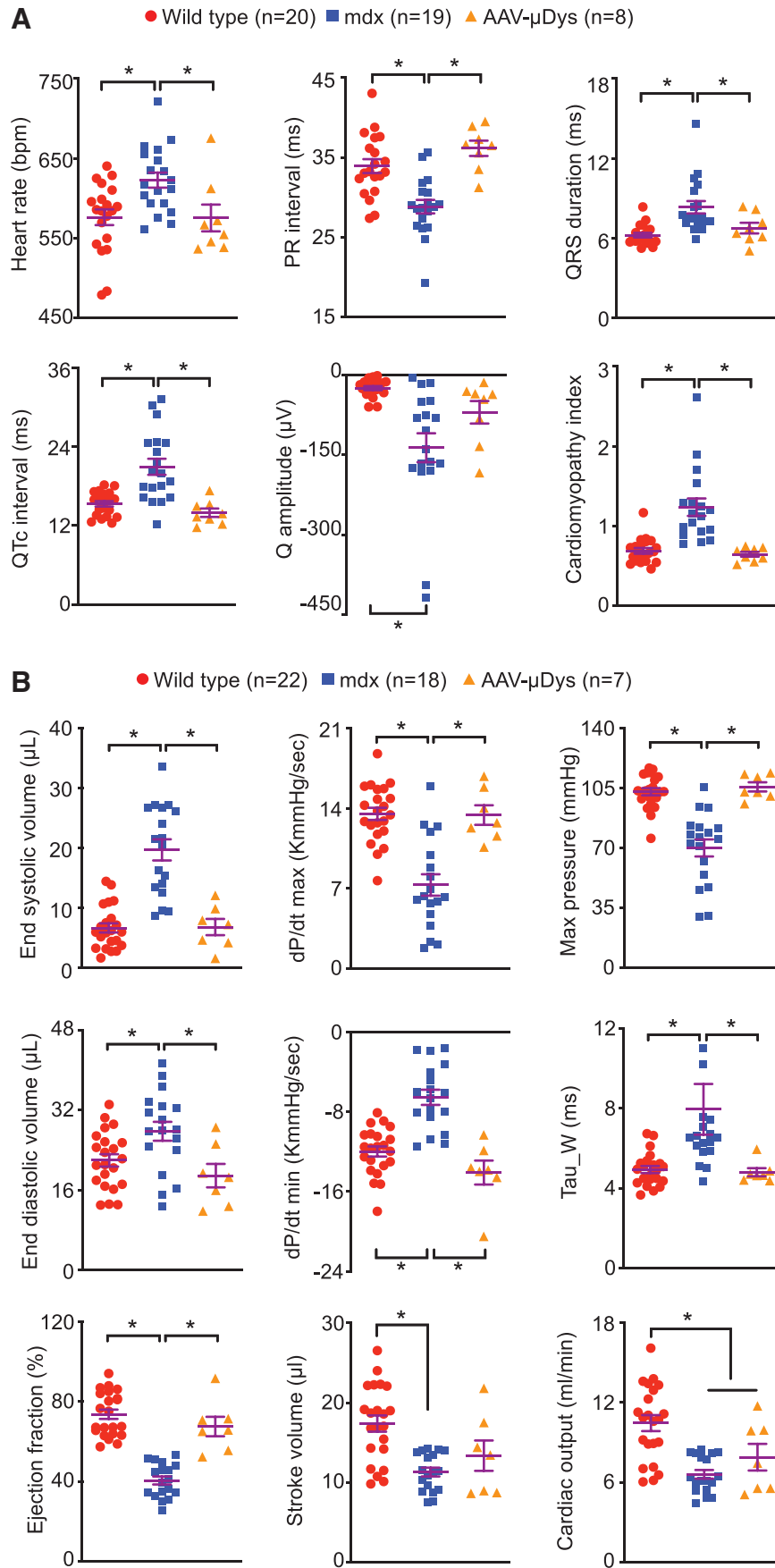


Figure 4. Long-term systemic AAV9.micro-dystrophin therapy resulted in persistent heart function improvement till 21 months of age. **(A)** Quantitative ECG parameters from WT, untreated mdx and AAV9.micro-dystrophin-treated mdx mice. **(B)** Quantitative cardiac pump function parameters from left-ventricular catheterization assay showing systolic (*top panel*), diastolic (*middle panel*) and overall heart pump function (*bottom panel*) indices from WT, untreated mdx and AAV9.micro-dystrophin-treated mdx mice. *Significantly different from the groups indicated, $p < 0.05$.

pressure, stroke work, pressure at the max value of dV/dt , pressure and volume at the maximum value of dP/dt , volume at the minimum value of dP/dt , and maximum power (Supplementary Table S1). Anatomical parameters of the treated heart (weights and weight ratios) showed a trend of improvement (Supplementary Table S2).

DISCUSSION

In this study, we evaluated lifelong systemic AAV μ Dys gene therapy in a mouse DMD model. We showed that a single treatment in young adult mdx mice resulted in persistent and robust μ Dys expression in skeletal muscle and heart till the mice reached the terminal age (Fig. 1; Supplementary Figs. S1 and S2). Gene therapy reduced fibrosis and inflammation in muscle and heart, lowered serum CK, and increased grip force and treadmill running (Figs. 2 and 3; Supplementary Fig. S3). Importantly, it significantly improved the electric and mechanical function of the heart and prevented dilated cardiomyopathy (Fig. 4; Supplementary Fig. S4 and Supplementary Table S1).

The size of the full-length dystrophin protein is 427 kD.² It contains four major domains, including the N-terminal domain, rod domain, cysteine-rich domain, and the C-terminal domain. The rod domain contains 24 spectrin-like repeats and four hinges. Patient studies suggest that highly truncated dystrophins can significantly reduce dystrophic phenotype.^{40,41} Based on clinical observations, abbreviated μ Dys genes were developed to fit into the AAV vector, the only viral vector that can efficiently deliver a transgene to all muscles in the body.⁴ A variety of μ Dys genes have been tested in rodent and canine DMD models. In most studies, the μ Dys AAV vector was delivered to young animals and the therapeutic effect was examined when the treated animals reached adulthood. In a subset of studies, the AAV μ Dys vector was administered to old animals and examined at their terminal age.^{42–44} However, lifelong therapy has not been examined.

There are two fundamental questions in DMD gene replacement therapy. First, whether permanent dystrophin expression is required for lifelong benefits. Second, whether it is possible to achieve permanent dystrophin expression from a single therapy. An RNA interference study found that persistent knockdown of dystrophin for 1 year did not cause muscle disease in adult mice.⁴⁵ However, when a floxed dystrophin gene was removed by Cre recombinase in adult mice, we observed significant dystrophic phenotype and function reduction in both skeletal muscle and heart.⁴⁶ Our data suggest that an effective DMD gene therapy depends on enduring dystrophin expression.

Several studies have shown that AAV vectors can persist in normal tissues, including muscle, for years.^{20,47} However, this may not be the case in a dystrophic muscle. Cordier *et al.* demonstrated immune-mediated AAV loss in dystrophic but not normal muscle, suggesting a dystrophic microenvironment may potentiate the cytotoxic T cell

response against the AAV vector.⁴⁸ Le Hir *et al.* found that leaky sarcolemma and muscle degeneration play critical roles in AAV loss from dystrophic muscle.⁴⁹ This is especially true when a nontherapeutic AAV vector was delivered or when therapeutic dystrophin restoration was suboptimal. Dupont *et al.* further showed that mRNA produced from the AAV vector was selectively damaged by oxidative stress in dystrophic muscle.⁵⁰ Several different strategies have been used to prevent AAV loss in dystrophic muscle.

The use of the muscle-specific promoter greatly reduced immunological AAV loss.⁴⁸ Pretreatment with antisense oligonucleotide mediated exon-skipping also effectively prevented AAV loss, likely due to transient stabilization of the sarcolemma by exon-skipping rescued dystrophin.^{51,52} A third approach is to prevent muscle degeneration and turnover.^{49,53} In our study, we achieved supraphysiological level saturated μ Dys expression. We believe this has effectively stopped AAV loss from degeneration-induced myofiber death. We would like to emphasize that our findings may not directly translate to human patients, because the level of μ Dys expression we saw in this study is hard to achieve in a clinical trial. Furthermore, the highly minimized μ Dys cannot fully protect muscle from damage induced by contraction, especially eccentric contraction.

A reduction of centrally nucleated myofibers is often used to evaluate μ Dys therapy.^{14,16,54} However, we did not see a statistically significant decrease in centronucleation, although a trend of reduction was noted (Fig. 2E). We believe this is likely due to the age of AAV injection rather than the ineffectiveness of the therapy. We delivered the AAV- μ Dys vector to 3-month-old mdx mice. At this age, mdx muscle disease has become stable.⁵⁵ Migration of the centrally located myonuclei to the peripheral is a lengthy process and may take up to 2 years.⁵⁶

Improved respiratory care (such as assisted ventilation) in the past several decades has unmasked cardiomyopathy as a leading cause of death in Duchenne patients. With this backdrop, we have paid special attention to cardiac rescue in our study. AAV μ Dys therapy has been evaluated in the heart of dystrophin-deficient rodents by many groups.^{42,43,57–64} These studies revealed correct sarcolemmal localization of μ Dys in cardiomyocytes, restoration of dystrophin-associated glycoprotein complex, prevention of Evans blue dye uptake, suppression of myocardial fibrosis, and improvements in electrocardiography and hemodynamic function. Interestingly, only H2 Dys (also called Δ R4-23/ Δ C μ Dys and M1 μ Dys) and its derivatives have been studied in the heart.

H2 μ Dys contains the N-terminal domain, H1, R1, R2, R3, H2, R24, H4, and the cysteine-rich domain. A recent proteomic study suggests that H2 μ Dys has an altered association with syntrophin and cavin in the heart.⁶⁵ Modified H2 μ Dys variants were investigated in two newly published studies. In one study, the authors examined H3 μ Dys. This μ Dys is identical to H2 μ Dys except for the replacement of H2 by H3. Similar to H2 μ Dys, H3 μ Dys effectively pre-

vented cardiac disease in a new DMD cardiomyopathy model.⁶⁴ In another study, the authors added different lengths of the C-terminal domain to H2 μ Dys.⁶³ The C-terminal domain has been implicated in heart protection in a genotype–phenotype correlation analysis.⁶⁶ However, no added cardiac benefits were observed in the new study.⁶³

Three different versions of μ Dys are currently in human trials (NCT03362502, NCT04281485, and NCT05429372 sponsored by Pfizer; NCT03368742 sponsored by Solid Biosciences; NCT03375164, NCT03769116, NCT04626674, and NCT05096221 sponsored by Sarepta; and EudraCT Number 2020-002093-27 sponsored by Genethon).¹⁹ They all contain the N-terminal domain and cysteine-rich domain. The major differences are (1) the number of spectrin-like repeats (four repeats in trials sponsored by Sarepta and Genethon, five repeats in trials sponsored by Pfizer and Solid Biosciences), and (2) with or without a central hinge (with a central hinge in trials sponsored by Pfizer, Sarepta, and Genethon; no central hinge in trials sponsored by Solid Biosciences).

Several trials used H2 μ Dys (NCT03375164, NCT03769116, NCT04626674, and NCT05096221 sponsored by Sarepta; EudraCT Number 2020-002093-27 sponsored by Genethon).^{67,68} However, other trials used μ Dys construct that does not carry hinge 2 (NCT03362502, NCT04281485, and NCT05429372 sponsored by Pfizer; NCT03368742 sponsored by Solid Biosciences).^{37–39} It is currently unclear whether μ Dys can protect the heart in the absence of a central hinge. To address this issue, we used a μ Dys gene similar to the one used in Solid Bioscience trial (NCT03368742).^{38,39}

Specifically, we replaced R2 and R3 of the R1-R2-R3 membrane-binding domain with R16 and R17,⁶⁹ the two repeats essential for anchoring neuronal nitric oxide synthase to the sarcolemma in skeletal muscle.^{34,70,71} Given the robust cardiac rescue observed in our study, we conclude that a central hinge is not required to protect the heart by μ Dys. In support, we recently found that a novel R16-19 containing μ Dys isoform completely normalized arrhythmia-inducing Na current abnormality in heart Purkinje fibers.¹⁷

We have previously studied cardiac protection of Δ H2-R19 mini-dystrophin in heart-specific transgenic mice.²⁸ Δ H2-R19 mini-dystrophin is two times larger than μ Dys used in this study. Interestingly, we detected better heart function rescue with μ Dys. We believe the improved protection is likely due to simultaneous treatment of both heart and skeletal muscle with systemic μ Dys therapy. Generation and analysis of Δ H2-R19 mini-dystrophin heart/skeletal muscle double transgenic mice will help to delineate whether larger dystrophin can better protect the heart.

Our study has several limitations. First, the study was not designed to evaluate the effect of systemic μ Dys therapy on the lifespan. Second, we only examined the long-term benefits in female mice. Third, we did not quantify the contractile properties of the skeletal muscle. Future studies are war-

ranted to determine whether μ Dys therapy can extend the lifespan, whether similar benefits can be achieved in male mdx mice, and whether lifelong μ Dys therapy improves the contractile properties of the limb muscle and diaphragm.^{28,72} Most importantly, there is an urgent need to investigate long-term μ Dys therapy in large animal models (such as dystrophin-deficient canines) because the canine model better recapitulates the clinical phenotype and is more suitable to investigate the immune response to AAV μ Dys therapy.⁷³

In summary, we demonstrated the lifelong benefits of a single systemic AAV μ Dys gene therapy in young mdx mice. Our findings provide additional support to continue μ Dys therapy in DMD patients.

AUTHORS' CONTRIBUTIONS

N.B.W. and D.D. conceived the idea and designed the study. N.B.W., Y.Y., B.H., and J.H.S., conducted experiments. N.B.W., A.S., G.Y., and D.D. analyzed the data. N.B.W., G.Y., and D.D. wrote the paper. A.S., G.Y., and D.D. edited the paper. A.S. and D.D. secured the funding. All authors approved the submission.

AUTHOR DISCLOSURE

D.D. is a member of the scientific advisory board for Solid Biosciences and equity holders of Solid Biosciences. D.D. is a member of the scientific advisory board for Sardocor Corp. D.D. is an inventor on several issued and filed patents on micro-dystrophin gene therapy and recombinant AAV vectors. The Duan lab received research support unrelated to this project from Solid Biosciences in the past 3 years. The Duan lab has received research support unrelated to this project from Edgewise Therapeutics in the past 3 years. A.S. is a cofounder of, and has equity in, Lacerta Therapeutics. He is also a consultant for Passage Bio and AgeX Therapeutics and an inventor on several issued and filed patents on recombinant AAV vectors that have been or are being licensed to various AAV gene therapy companies.

FUNDING INFORMATION

This study was supported by grants from the National Institutes of Health (AR-70517 to D.D.; AR-81018 to A.S. and D.D.), Jesse Davidson Foundation-Defeat Duchenne Canada (to D.D.), Jett Foundation (to D.D.), and Jackson Freeland DMD Research Fund (to D.D.). B.H. was supported by the University of Missouri Life Science Fellowship.

SUPPLEMENTARY MATERIAL

Supplementary Figure S1
Supplementary Figure S2
Supplementary Figure S3
Supplementary Figure S4
Supplementary Table S1
Supplementary Table S2

REFERENCES

1. Duan D. Micro-dystrophin gene therapy goes systemic in Duchenne muscular dystrophy patients. *Hum Gene Ther* 2018;29:733–736.
2. Duan D, Goemans N, Takeda S, et al. Duchenne muscular dystrophy. *Nat Rev Dis Primers* 2021; 7:13.
3. Kunkel LM. 2004 William Allan award address. cloning of the DMD gene. *Am J Hum Genet* 2005; 76:205–214.
4. Duan D. Systemic delivery of adeno-associated viral vectors. *Curr Opin Virol* 2016;21:16–25.
5. Verhaart IEC, Aartsma-Rus A. Therapeutic developments for Duchenne muscular dystrophy. *Nat Rev Neurol* 2019;15:373–386.
6. Mendell JR, Al-Zaidy S, Shell R, et al. Single-dose gene-replacement therapy for spinal muscular atrophy. *N Engl J Med* 2017;377:1713–1722.
7. Carter BJ. Adeno-associated virus and the development of adeno-associated virus vectors: a historical perspective. *Mol Ther* 2004;10:981–989.
8. Wang D, Tai PWL, Gao GP. Adeno-associated virus vector as a platform for gene therapy delivery. *Nat Rev Drug Discov* 2019;18:358–378.
9. Li C, Samulski RJ. Engineering adeno-associated virus vectors for gene therapy. *Nat Rev Genet* 2020;21:255–272.
10. Lai Y, Yue Y, Duan D. Evidence for the failure of adeno-associated virus serotype 5 to package a viral genome > or = 8.2 kb. *Mol Ther* 2010;18:75–79.
11. Lostal W, Kodippili K, Yue Y, et al. Full-length dystrophin reconstitution with adeno-associated viral vectors. *Hum Gene Ther* 2014;25:552–562.
12. Scott J, Li S, Harper S, et al. Viral vectors for gene transfer of micro-, mini-, or full-length dystrophin. *Neuromuscul Disord* 2002;12 Suppl:S23.
13. Duan D. From the smallest virus to the biggest gene: marching towards gene therapy for Duchenne muscular dystrophy. *Discov Med* 2006;6:103–108.
14. Wang B, Li J, Xiao X. Adeno-associated virus vector carrying human minidystrophin genes effectively ameliorates muscular dystrophy in mdx mouse model. *Proc Natl Acad Sci U S A* 2000;97: 13714–13719.
15. Harper SQ, Hauser MA, DelloRusso C, et al. Modular flexibility of dystrophin: implications for gene therapy of Duchenne muscular dystrophy. *Nat Med* 2002;8:253–261.
16. Ramos JN, Hollinger K, Bengtsson NE, et al. Development of novel micro-dystrophins with enhanced functionality. *Mol Ther* 2019;27:623–635.
17. Ebner J, Pan X, Yue Y, et al. Microdystrophin therapy rescues impaired Na currents in cardiac Purkinje fibers from dystrophin-deficient Mdx mice. *Circ Arrhythm Electrophysiol* 2022;15:e011161.
18. Wasala LP, Watkins T, Wasala N, et al. The implication of hinge 1 and hinge 4 in micro-dystrophin gene therapy for Duchenne muscular dystrophy. *Hum Gene Ther* 2022 [Epub ahead of print]; DOI: 10.1089/hum.2022.180
19. Duan D. Systemic AAV micro-dystrophin gene therapy for Duchenne muscular dystrophy. *Mol Ther* 2018;26:2337–2356.
20. Buchlis G, Podsakoff GM, Radu A, et al. Factor IX expression in skeletal muscle of a severe hemophilia B patient 10 years after AAV-mediated gene transfer. *Blood* 2012;119:3038–3041.
21. Chamberlain JS, Metzger J, Reyes M, et al. Dystrophin-deficient mdx mice display a reduced life span and are susceptible to spontaneous rhabdomyosarcoma. *Faseb J* 2007;21:2195–2204.
22. Li D, Long C, Yue Y, et al. Sub-physiological sargoglycan expression contributes to compensatory muscle protection in mdx mice. *Hum Mol Genet* 2009;18:1209–1220.
23. Bostick B, Yue Y, Long C, et al. Prevention of dystrophin-deficient cardiomyopathy in twenty-one-month-old carrier mice by mosaic dystrophin expression or complementary dystrophin/utrophin expression. *Circ Res* 2008;102:121–130.
24. Bostick B, Yue Y, Duan D. Gender influences cardiac function in the mdx model of Duchenne cardiomyopathy. *Muscle Nerve* 2010;42:600–603.
25. Shin J-H, Pan X, Hakim CH, et al. Microdystrophin ameliorates muscular dystrophy in the canine model of Duchenne muscular dystrophy. *Mol Ther* 2013;21:750–757.
26. Shin J-H, Yue Y, Duan D. Recombinant adeno-associated viral vector production and purification. *Methods Mol Biol* 2012;798:267–284.
27. Bostick B, Yue Y, Long C, et al. Cardiac expression of a mini-dystrophin that normalizes skeletal muscle force only partially restores heart function in aged mdx mice. *Mol Ther* 2009;17:253–261.
28. Hakim CH, Li D, Duan D. Monitoring murine skeletal muscle function for muscle gene therapy. *Methods Mol Biol* 2011;709:75–89.
29. Bostick B, Yue Y, Duan D. Phenotyping cardiac gene therapy in mice. *Methods Mol Biol* 2011;709:91–104.
30. Duan D, Rafael-Fortney JA, Blain A, et al. Standard operating procedures (SOPs) for evaluating the heart in preclinical studies of Duchenne muscular dystrophy. *J Cardiovasc Transl Res* 2016;9:85–86.
31. Parent project muscular dystrophy. Standard operating procedures (sops) for Duchenne animal models. Washington, DC; 2023. Available from <https://www.parentprojectmd.org/research/for-researchers-industry/resources/standard-operating-procedures-for-duchenne-animal-models/> [Last accessed: April 17, 2023].
32. Weiss JL, Frederiksen JW, Weisfeldt ML. Hemodynamic determinants of the time-course of fall in canine left ventricular pressure. *J Clin Invest* 1976;58:751–760.
33. Cheung MC, Spalding PB, Gutierrez JC, et al. Body surface area prediction in normal, hypermuscular, and obese mice. *J Surg Res* 2009;153:326–331.
34. Lai Y, Thomas GD, Yue Y, et al. Dystrophins carrying spectrin-like repeats 16 and 17 anchor nNOS to the sarcolemma and enhance exercise performance in a mouse model of muscular dystrophy. *J Clin Invest* 2009;119:624–635.
35. Li D, Yue Y, Lai Y, et al. Nitrosative stress elicited by nNOSmu delocalization inhibits muscle force in dystrophin-null mice. *J Pathol* 2011;223:88–98.
36. Yue Y, Pan X, Hakim CH, et al. Safe and bodywide muscle transduction in young adult Duchenne muscular dystrophy dogs with adeno-associated virus. *Hum Mol Genet* 2015;24:5880–5890.
37. Moorehead T, Yong F, Neelakantan S, et al. Safety and tolerability of PF-06939926 in ambulatory boys with Duchenne muscular dystrophy: a phase 1b Multicenter, Open-Label, Dose Ascending Study. *Mol Ther* 2020;28:S273–S274.
38. Gonzalez JP, Brown KJ, Lawlor MW, et al. SGT-001 microdystrophin gene therapy for Duchenne muscular dystrophy. *Mol Ther* 2020;28:S220.
39. Morris CA, Dregghici RD, Redican S, et al. IGNITE DMD study of SGT-001 microdystrophin gene therapy for Duchenne muscular dystrophy: long-term outcomes and biomarker update. *Mol Ther* 2022;30:S553–S554.
40. England SB, Nicholson LV, Johnson MA, et al. Very mild muscular dystrophy associated with the deletion of 46% of dystrophin. *Nature* 1990;343:180–182.
41. Beggs AH, Hoffman EP, Snyder JR, et al. Exploring the molecular basis for variability among patients with Becker muscular dystrophy: dystrophin gene and protein studies. *Am J Hum Genet* 1991;49:54–67.
42. Bostick B, Shin J-H, Yue Y, et al. AAV-microdystrophin therapy improves cardiac performance in aged female mdx mice. *Mol Ther* 2011; 19:1826–1832.
43. Bostick B, Shin J-H, Yue Y, et al. AAV micro-dystrophin gene therapy alleviates stress-induced cardiac death but not myocardial fibrosis in >21-m-old mdx mice, an end-stage model of Duchenne muscular dystrophy cardiomyopathy. *J Mol Cell Cardiol* 2012;53:217–222.
44. Gregorevic P, Blankinship MJ, Allen JM, et al. Systemic microdystrophin gene delivery improves skeletal muscle structure and function in old dystrophic mdx mice. *Mol Ther* 2008;16:657–664.
45. Ghahramani Seno MM, Graham IR, Athanaspoulos T, et al. RNAi-mediated knockdown of dystrophin expression in adult mice does not lead to overt muscular dystrophy pathology. *Hum Mol Genet* 2008;17:2622–2632.
46. Wasala NB, Lai Y, Shin J-H, et al. Genomic removal of a therapeutic mini-dystrophin gene from adult mice elicits a Duchenne muscular dystrophy-like phenotype. *Hum Mol Genet* 2016;25:2633–2644.

47. Stieger K, Schroeder J, Provost N, et al. Detection of intact rAAV particles up to 6 years after successful gene transfer in the retina of dogs and primates. *Mol Ther* 2009;17:516–523.
48. Cordier L, Gao GP, Hack AA, et al. Muscle-specific promoters may be necessary for adeno-associated virus-mediated gene transfer in the treatment of muscular dystrophies. *Hum Gene Ther* 2001;12:205–215.
49. Le Hir M, Goyenvallé A, Peccate C, et al. AAV genome loss from dystrophic mouse muscles during AAV-U7 snRNA-mediated exon-skipping therapy. *Mol Ther* 2013;21:1551–1558.
50. Dupont JB, Tournaire B, Georget C, et al. Short-lived recombinant adeno-associated virus transgene expression in dystrophic muscle is associated with oxidative damage to transgene mRNA. *Mol Ther Methods Clin Dev* 2015;2:15010.
51. Peccate C, Mollard A, Le Hir M, et al. Antisense pretreatment increases gene therapy efficacy in dystrophic muscles. *Hum Mol Genet* 2016;25:3555–3563.
52. Forand A, Muchir A, Mougénot N, et al. Combined treatment with peptide-conjugated phosphorodiamidate morpholino oligomer-PPMO and AAV-U7 rescues the severe DMD phenotype in mice. *Mol Ther Methods Clin Dev* 2020;17:695–708.
53. Pacak CA, Conlon T, Mah CS, et al. Relative persistence of AAV serotype 1 vector genomes in dystrophic muscle. *Genet Vaccines Ther* 2008;6:14.
54. Liu M, Yue Y, Harper SQ, et al. Adeno-associated virus-mediated microdystrophin expression protects young mdx muscle from contraction-induced injury. *Mol Ther* 2005;11:245–256.
55. McGreevy JW, Hakim CH, McIntosh MA, et al. Animal models of Duchenne muscular dystrophy: from basic mechanisms to gene therapy. *Dis Model Mech* 2015;8:195–213.
56. Meyer GA. Evidence of induced muscle regeneration persists for years in the mouse. *Muscle Nerve* 2018;58:858–862.
57. Yue Y, Li Z, Harper SQ, et al. Microdystrophin gene therapy of cardiomyopathy restores dystrophin-glycoprotein complex and improves sarcolemma integrity in the mdx mouse heart. *Circulation* 2003;108:1626–1632.
58. Bostick B, Yue Y, Lai Y, et al. Adeno-associated virus serotype-9 microdystrophin gene therapy ameliorates electrocardiographic abnormalities in mdx mice. *Hum Gene Ther* 2008;19:851–856.
59. Gregorevic P, Allen JM, Minami E, et al. rAAV6-microdystrophin preserves muscle function and extends lifespan in severely dystrophic mice. *Nat Med* 2006;12:787–789.
60. Townsend D, Blankinship MJ, Allen JM, et al. Systemic administration of micro-dystrophin restores cardiac geometry and prevents dobutamine-induced cardiac pump failure. *Mol Ther* 2007;15:1086–1092.
61. Shin J-H, Nitahara-Kasahara Y, Hayashita-Kinoh H, et al. Improvement of cardiac fibrosis in dystrophic mice by rAAV9-mediated microdystrophin transduction. *Gene Ther* 2011;18:910–919.
62. Malerba A, Sidoli C, Lu-Nguyen N, et al. Dose-dependent microdystrophin expression enhancement in cardiac muscle by a cardiac-specific regulatory element. *Hum Gene Ther* 2021;32:1138–1146.
63. Bourdon A, Francois V, Zhang L, et al. Evaluation of the dystrophin carboxy-terminal domain for micro-dystrophin gene therapy in cardiac and skeletal muscles in the DMD(mdx) rat model. *Gene Ther* 2022;29:520–535.
64. Howard ZM, Dorn LE, Lowe J, et al. Micro-dystrophin gene therapy prevents heart failure in an improved Duchenne muscular dystrophy cardiomyopathy mouse model. *JCI Insight* 2021;6:e146511.
65. Wang H, Marrosu E, Brayson D, et al. Proteomic analysis identifies key differences in the cardiac interactomes of dystrophin and micro-dystrophin. *Hum Mol Genet* 2021;30:1321–1336.
66. Tandon A, Jefferies JL, Villa CR, et al. Dystrophin genotype-cardiac phenotype correlations in Duchenne and Becker muscular dystrophies using cardiac magnetic resonance imaging. *Am J Cardiol* 2015;115:967–971.
67. Mendell JR, Sahenk Z, Lehman K, et al. Assessment of systemic delivery of rAAVrh74.MHCK7.microdystrophin in children with Duchenne muscular dystrophy: a nonrandomized controlled trial. *JAMA Neurol* 2020;77:1122–1131.
68. Genethon. Genethon announces first patient dosed in clinical trial of investigational gene therapy GNT 0004 for Duchenne muscular dystrophy. https://www.genethon.fr/wp-content/uploads/2021/04/PR_GENETHON_DMD-1.pdf (last accessed April 20, 2021).
69. Zhao J, Kodippili K, Yue Y, et al. Dystrophin contains multiple independent membrane-binding domains. *Hum Mol Genet* 2016;25:3647–3653.
70. Lai Y, Zhao J, Yue Y, et al. alpha2 and alpha3 helices of dystrophin R16 and R17 frame a microdomain in the alpha1 helix of dystrophin R17 for neuronal NOS binding. *Proc Natl Acad Sci U S A* 2013;110:525–530.
71. Li D, Bareja A, Judge L, et al. Sarcolemmal nNOS anchoring reveals a qualitative difference between dystrophin and utrophin. *J Cell Sci* 2010;123:2008–2013.
72. Hakim CH, Lessa TB, Jenkins GJ, et al. An improved method for studying mouse diaphragm function. *Sci Rep* 2019;9:19453.
73. Duan D. Duchenne muscular dystrophy gene therapy in the canine model. *Hum Gene Ther Clin Dev* 2015;26:57–69.

Received for publication September 17, 2022;
accepted after revision December 2, 2022.

Published online: December 13, 2022.